Biochimica et Biophysica Acta 1818 (2012) 762–775

Contents lists available at SciVerse ScienceDirect

Biochimica et Biophysica Acta

journal homepage: www.elsevier.com/locate/bbamem

Structural and biophysical characterization of an antimicrobial peptide chimera comprised of lactoferricin and lactoferrampin

Evan F. Haney [a], Kamran Nazmi [b], Jan G.M. Bolscher [b], Hans J. Vogel [a,*]

[a] Biochemistry Research Group, Department of Biological Sciences, University of Calgary, Calgary, Alberta, Canada
[b] Academic Centre for Dentistry Amsterdam, Free University Amsterdam, Department of Oral Biochemistry, The Netherlands

ARTICLE INFO

Article history:
Received 3 October 2011
Received in revised form 21 November 2011
Accepted 23 November 2011
Available online 3 December 2011

Keywords:
Antimicrobial peptide
Lactoferricin
Lactoferrampin
NMR solution structure
Peptide–membrane interactions

ABSTRACT

Lactoferricin and lactoferrampin are two antimicrobial peptides found in the N-terminal lobe of bovine lactoferrin with broad spectrum antimicrobial activity against a range of Gram-positive and Gram-negative bacteria as well as *Candida albicans*. A heterodimer comprised of lactoferrampin joined to a fragment of lactoferricin was recently reported in which these two peptides were joined at their C-termini through the two amino groups of a single Lys residue (Bolscher et al., 2009, Biochimie 91(1):123–132). This hybrid peptide, termed LFchimera, has significantly higher antimicrobial activity compared to the individual peptides or an equimolar mixture of the two. In this work, the underlying mechanism behind the increased antibacterial activity of LFchimera was investigated. Differential scanning calorimetry studies demonstrated that all the peptides influenced the thermotropic phase behaviour of anionic phospholipid suspensions. Calcein leakage and vesicle fusion experiments with anionic liposomes revealed that LFchimera had enhanced membrane perturbing properties compared to the individual peptides. Peptide structures were evaluated using circular dichroism and NMR spectroscopy to gain insight into the structural features of LFchimera that contribute to the increased antimicrobial activity. The NMR solution structure, determined in a miscible co-solvent mixture of chloroform, methanol and water, revealed that the Lys linkage increased the helical content in LFchimera compared to the individual peptides, but it did not fix the relative orientations of lactoferricin and lactoferrampin with respect to each other. The structure of LFchimera provides insight into the conformation of this peptide in a membranous environment and improves our understanding of its antimicrobial mechanism of action.

1. Introduction

The majority of biophysical studies concerning antimicrobial peptides published to date focus on a variety of experiments performed on highly purified peptide samples in an effort to characterize the antimicrobial mode of action of a single peptide [1]. A recent trend has seen the emergence of reports that focus on the combined effects of antimicrobial peptides wherein a mixture of peptides, administered together, cause a more substantial antimicrobial effect [2–4]. The concept of synergy between antimicrobial peptides is rapidly gaining momentum as researchers seek to enhance the antimicrobial activity and effectiveness of peptide sequences [5]. The combined effect of multiple antimicrobial peptides has inspired the generation of unique hybrid antimicrobial peptides in which peptides are covalently linked to each other to generate molecules with enhanced antimicrobial activity. An example of such a hybrid peptide is the disulphide-linked magainin-PGLa heterodimer [6] for which we recently published the micelle bound structure [7]. In the present work, the structure and membrane perturbing properties of a novel hybrid peptide comprised of two antimicrobial sequences obtained from the intact bovine lactoferrin protein is evaluated and compared to each of the component peptides. A unique feature of this peptide chimera is that the two peptides are covalently joined at their C-termini through the two amino groups of a single lysine residue.

Lactoferrin is an 80 kDa iron binding protein found in the secretory fluids of mammals. In addition to its well-documented ability to bind iron, which contributes directly to its antibacterial properties by sequestering iron required for bacterial growth [8, 9], lactoferrin also possesses a wide range of biological functions (unrelated to iron binding) including antibacterial, antiviral, anticancer and immunomodulatory activities [10–12]. Of particular interest to antimicrobial peptide researchers is the cationic N-terminal lobe of bovine lactoferrin which includes two antimicrobial sequences, lactoferricin and lactoferrampin (Fig. 1).

Abbreviations: COSY, Correlation spectroscopy; DPPG, 1,2-dihexadecanoyl-sn-glycero-3-phospho-(1′-rac-glycerol); DSC, Differential scanning calorimetry; ePE, egg derived phosphatidylethanolamine; ePG, egg derived phosphatidylglycerol; LFampB, Bovine lactoferrampin; LFchimera, Lys linked LFcin17–30 and LFampB heterodimer; LFcin, Lactoferricin; LUV, Large unilamellar vesicle; NMR, Nuclear magnetic resonance; NOESY, Nuclear Overhauser spectroscopy; PLE, *E. coli* polar lipid extract; RMSD, Root mean squared deviation; SDS, Sodium dodecyl sulphate; TOCSY, Total correlation spectroscopy

* Corresponding author at: Department of Biological Sciences, University of Calgary, 2500 University Drive NW, Calgary, Alberta, Canada, T2N 1N4. Tel.: +1 403 220 6006.
E-mail address: vogel@ucalgary.ca (H.J. Vogel).

0005-2736/$ – see front matter © 2011 Elsevier B.V. All rights reserved.
doi:10.1016/j.bbamem.2011.11.023

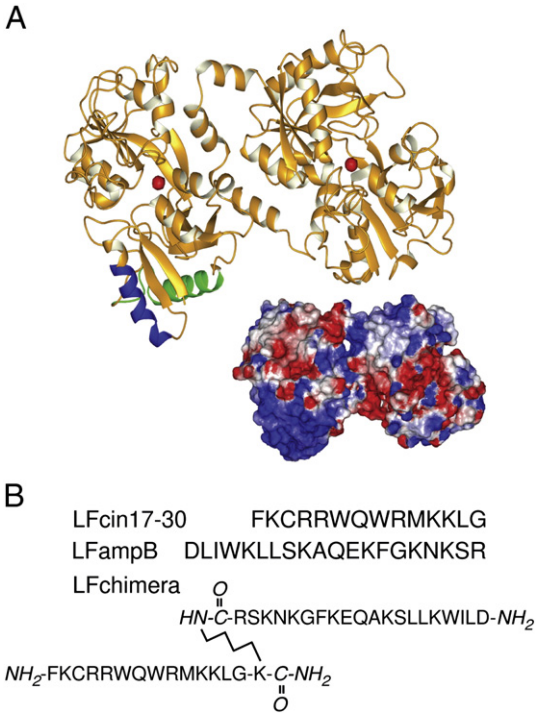

Fig. 1. Crystal structure of bovine lactoferrin (PDB ID = 1BLF, A). Each lobe of lactoferrin is capable of binding to one iron atom, shown in red. Bovine lactoferrin is the source of two antimicrobial peptides, lactoferricin and lactoferrampin. LFcin17–30 (blue) and LFampB (green) are found in the highly cationic N-terminal lobe of bovine lactoferrin as seen in the space filling model of the protein with positively charged regions coloured in blue, negatively charged regions in red and neutral regions appearing white. The sequences of the two peptides, as well as the unique sequence of LFchimera, in which the two peptides are joined through a single Lys residue, are shown in (B). Joining these two peptides through a single lysine residue makes it possible for these sequences to maintain a relative orientation with respect to each other, similar to that seen in the crystal structure of bovine lactoferrin.

Lactoferricin (LFcin), is an antimicrobial peptide that has been extensively studied by several groups, including our own. LFcins are released from lactoferrin by the proteolytic activity of pepsin in the gut [13–15]. These polypeptides display significantly higher antibacterial activity compared to the intact lactoferrin protein and considerable effort has gone into elucidating their mechanism of action [16]. Bovine LFcin corresponds to residues 17–41 of lactoferrin and it forms an amphipathic β-sheet hairpin structure in aqueous solution [17] that is distinct from the α-helical conformation seen in the corresponding sequence in the crystal structure of bovine lactoferrin [18]. Shorter versions of bovine LFcin retain much of the antimicrobial activity of the native peptide and these truncated forms have provided detailed structural, functional and biophysical insights into the interaction between LFcin and lipid bilayers or bacterial cells [19–24].

Bovine lactoferrampin (LFampB) is an antimicrobial peptide identified through sequence analysis of bovine lactoferrin [24] with broad range antimicrobial activity against a variety of Gram-positive and Gram-negative bacteria as well as candidacidal activity [25–28]. Freeze-fracture transmission electron microscopy of *E. coli* and *C. albicans* cells treated with LFampB revealed that the peptide causes partial disintegration of the plasma membrane [29], suggesting that the primary target of lactoferrampin is the cytoplasmic membrane.

The solution structures and membrane interactions of bovine and human lactoferrampins have been extensively characterized [30–32]. Like many antimicrobial peptides, lactoferrampin is unstructured in aqueous solution and it only adopts a helical conformation in the presence of lipids. The sodium dodecyl sulphate (SDS) micelle-bound NMR solution structure of lactoferrampin revealed an amphipathic helix in the N-terminal region of the peptide, while the cationic C-terminal region is devoid of regular secondary structure. Interestingly, removal of the positive charges in the C-terminal region decreases the antimicrobial potency of the peptide [26, 28] and adding positive charges to this region increases the antimicrobial activity [32]. Based on these results, a model of antimicrobial activity has been described wherein the cationic C-terminal region mediates the initial attraction of lactoferrampin to the negatively charged bacterial surface. This electrostatic attraction brings lactoferrampin into close proximity to the bacterial membrane, allowing for folding and insertion of the N-terminal helix into the bilayer, ultimately leading to membrane perturbation and cell death.

In the present work, the antimicrobial mechanism of action of a unique hybrid antimicrobial peptide composed of LFampB and LFcin17–30 is examined. The heterodimeric peptide (named LFchimera) is coupled together through the two amino groups of a single lysine residue at the C-terminal ends of both constituent peptides. In addition, the carboxyl group on the lysine linker is amidated to remove the negative charge (Fig. 1B). The rationale behind the design of the LFchimera was to link these two peptides in a manner that could maintain their relative orientation as seen in the crystal structure of bovine lactoferrin [18]. Since many of the biological host-defence activities of lactoferrin are localized in the cationic N-terminal lobe of the protein, it was hypothesized that joining LFampB to LFcin through this Lys linker might maintain the spatial orientation of these two sequences and enhance the activity of this heterodimer. Indeed, extensive characterization of the activity of LFchimera has shown it to be remarkably more potent against Gram-positive and Gram-negative bacteria compared to either of the constituent peptides [33, 34]. Additionally, the LFchimera has been found to possess antiparasitic activity [35] and even antibiotic resistant strains of *Staphylococcus aureus* and *Escherichia coli* are susceptible to this hybrid peptide [36]. Together, these studies highlight the potential of LFchimera as a future treatment option for serious bacterial infections. However, the structure of LFchimera and the molecular mechanisms underlying the enhanced antimicrobial activity remain to be elucidated.

In the present work, the effect of the peptides on the thermotropic phase behaviour of anionic phospholipids was examined using differential scanning calorimetry (DSC) [37]. Furthermore, the membrane perturbing properties of LFchimera and its constituent peptides was evaluated by monitoring the release of the self quenching dye, calcein, from large unilamellar vesicles (LUVs) of varying lipid composition. Peptide induced liposome fusion was also assessed as this is a feature that has previously been reported for the full length bovine LFcin peptide [38]. Structural characterization of all the peptides was performed using circular dichroism (CD) spectroscopy and high resolution nuclear magnetic resonance (NMR) spectroscopy. The results presented here reveal that the LFchimera has a stronger membrane perturbing effect than either LFampB or LFcin17–30 or a mixture of these two peptides. The CD and NMR structural results demonstrate that the LFchimera has increased helical content compared to the two constituent peptides, suggesting that the Lys linkage influences the structure of the LFampB and LFcin17–30 regions of LFchimera. The outcome of these experiments is discussed with respect to the previously reported antimicrobial activity of LFampB, LFcin17–30 and LFchimera. In addition, the merits of using a co-solvent mixture as a mimic for biological membranes in NMR spectroscopy are also considered.

2. Methods and materials

2.1. Peptide synthesis

Synthesis of LFcin17–30 and LFampB was performed in the same manner as described previously [29, 32]. The synthesis of LFchimera

was first described by Bolscher et al. [33] and was accomplished using special precursors from NovaBiochem (Now EMD Chemicals, Gibbstown, NJ). Briefly, synthesis was started by coupling Fmoc-Lys(ivDde)-OH to NovaSyn®TGR resin followed by the synthesis of LFcin17–30, terminated with *N*-α-t-BOC-protected Phe. Next, the ivDde-protecting group on the C-terminal Lys side chain was released by hydrazinolysis followed by the synthesis of LFampB. In this manner the LFchimera peptide comprises a single C-terminal lysine-amide substituted at the α- and ε-amino groups with the two peptides via the C-terminal site, while leaving the two N-termini as free ends. All peptides were purified with RP-HPLC (Jasco Inc. Easton, MD) to at least 95% purity and their identity was confirmed with ion trap mass spectrometry.

2.2. Preparation of lipid vesicles

Stock chloroform lipid solutions of egg derived phosphatidylglycerol (ePG), egg phosphatidylethanolamine (ePE) and *E. coli* polar lipid extract (PLE) were obtained from Avanti Polar Lipids (Alabaster, AL). Briefly, the necessary volume of stock lipid solution was added to a glass vial and the chloroform solvent was evaporated in a stream of nitrogen gas. The vial was then placed under vacuum for ~2 h to remove all traces of the organic solvent. Large unilamellar vesicles (LUVs) composed of 3:1 and 1:1 ratios of ePE:ePG as well as PLE were prepared according to Schibli et al., [39]. To prepare calcein encapsulated LUVs, the dried lipid film was resuspended in Tris buffer (10 mM Tris, 150 mM NaCl, 1 mM EDTA, pH 7.4) containing 70 mM calcein. The lipid suspension was freeze-thawed five times using liquid nitrogen followed by 15 passes through two 0.1 μm polycarbonate filters (Nucleopore Filtration Products, Pleasonton, CA) using a mini-extruder apparatus (Avanti Polar Lipids, Alabaster, AL) to generate LUVs. The calcein containing LUVs were separated from free calcein using a Sephadex G-50 superfine gel-filtration column. Calcein encapsulated LUVs were visually collected as the first strong yellow fraction to elute from the column. Liposomes used in the fusion assays were prepared by sonicating the lipid suspension for ~1 h until the lipid suspension clarified. The concentration of lipid in all the samples was determined using the Ames phosphate assay [40], performed in triplicate.

2.3. Differential scanning calorimetry

The effect of the peptides on the thermotropic phase behaviour of 1,2-dihexadecanoyl-*sn*-glycero-3-phospho-(1′-*rac*-glycerol) (DPPG, Avanti Polar Lipids, Alabaster, AL) phospholipids was examined using differential scanning calorimetry (DSC) according to a modified protocol described by Prenner et al. [41]. Briefly, a 1 mg lipid film was prepared in a glass vial by evaporating the organic solvent from an appropriate volume of a chloroform stock solution of DPPG under a stream of nitrogen gas. The vial was incubated under vacuum for ~2 h and then stored at −20 °C until needed. The lipid film was heated to 60 °C and warm Tris buffer (10 mM Tris, 150 mM NaCl, 1 mM EDTA, pH 7.4) was added, followed by vigorous vortexing to resuspend all the lipid. Aqueous peptide solutions of LFcin17–30, LFampB and LFchimera were added to the lipid suspensions to achieve molar peptide:lipid ratios of 1:100, 1:50 and 1:10. The final concentration of DPPG in each DSC sample was 1.0 mg/ml.

The DSC experiments were carried out on degassed lipid samples using a Microcal high sensitivity VP-DSC (GE Healthcare, Piscatawy, NJ). Five heating scans between 20 and 60 °C were recorded for each sample using a scan rate of 10 °C/h. In all cases, the fourth and fifth heating scans were identical, indicating that the peptide had equilibrated amongst the lipid molecules. The fifth heating scan was used in the final analysis, performed with the Microcal Origin Software (version 7.0).

2.4. Calcein leakage

Calcein release from calcein encapsulated LUVs was monitored using a Varian Cary Eclipse Fluorimeter (Varian Inc. Palo Alto, CA.). Calcein containing LUVs were added to a final lipid concentration of 10 μM and the fluorescence intensity at 520 nm (excitation 490 nm) was measured for 1 min. After 1 min, the peptide was added to a final concentration of 1 μM (peptide:lipid ratio of 1:10) and the fluorescence emission was monitored for 10 min. At this point, 20 μl of 1% Triton X-100 was added to solubilise all of the LUVs and the fluorescence was monitored for another 1.5 min. Peptide to lipid molar ratios of 1:20, 1:30, 1:50 and 1:100 were tested by adjusting the amount of peptide added to the calcein LUV solutions. Solutions of LFampB, LFcin17–30, LFchimera and a mixture of the two constituent peptides were evaluated for their ability to induce calcein leakage. The % leakage of calcein was calculated using the following equation:

$$\%leakage = 100 \times (I - I_o)/(I_t - I_o)$$

where I is the fluorescence intensity 10 min after the addition of peptide, I_o is the fluorescence intensity prior to the addition of peptide and I_t is the intensity after the addition of triton. All calcein leakage experiments were performed in triplicate.

2.5. Liposome fusion

Peptide induced fusion of liposomes was examined by monitoring the change in absorbance of a peptide and liposome solution at 400 nm. An increase in the absorbance value at 400 nm is indicative of vesicle fusion [38, 42]. The absorbance of an ePE:ePG liposome solution (lipid concentration of 0.1 mM) was measured after 15 min of incubation with each peptide. Molar peptide to lipid ratios of 1:100, 1:50, 1:20 and 1:10 were tested and the experiments were performed in triplicate. In addition, the particle size of these same liposome solutions were monitored using a DynaPro dynamic light scattering instrument (Wyatt Technology Corporation, Santa Barbara, CA) to confirm the results of the liposome fusion assay (data not shown).

2.6. Circular dichroism spectroscopy

Circular dichroism spectra were acquired on a Jasco J-810 spectropolarimeter (Jasco, Inc. Easton, MD). 50 μM peptide samples in buffer (10 mM Tris, 150 mM NaCl, 1 mM EDTA, pH 7.4) and in buffered 200 mM SDS were collected at room temperature between 190 and 260 nm using a 1 mm pathlength cuvette. Additional samples containing a mixture of LFcin17–30 and LFampB, each at a concentration of 50 μM, were also recorded under the same conditions. Ellipticity values were recorded every 0.1 nm at a wavelength scanning speed of 200 nm/min. The response time was set to 0.5 s and the bandwidth was set to 1 nm. The final spectrum represents the accumulated average of 10 consecutive scans. The raw data was converted to mean residue ellipticity (MRE) according to [43] using the formula:

$$MRE = (\theta \times 0.1 \times MRW)/cl$$

where θ is the measured ellipticity in mdeg, c is the concentration in mg/ml, l is the cuvette pathlength in cm and MRW is the mean residue weight of the peptide. MRW is defined as:

$$MRW = MW/(n-1)$$

where MW is the molecular weight of the peptide in daltons and n is the number of residues in the peptide.

2.7. NMR spectroscopy

Approximately 1 mg of peptide was dissolved in 500 μl of a 4:4:1 co-solvent mixture of $CDCl_3$: methanol-*d3*: H_2O. The sample was transferred to an NMR tube and immediately flame sealed to prevent evaporation of the organic solvents. This co-solvent has been used previously as a membrane mimetic to examine the solution structures of other antimicrobial peptides [15, 44].

Two dimensional NOESY, TOCSY and COSY spectra were collected at 298°K on a Bruker Avance 600 MHz spectrometer for all of the peptide samples. To improve spectral resolution for the LFchimera sample, spectra were also acquired on a Bruker Avance 700 MHz spectrometer. Mixing times used in the NOESY experiments were 0.25 s on the 600 MHz and 0.5 s on the 700 MHz spectrometer. For the TOCSY experiments, mixing times of 0.1 and 0.12 s were used for the 600 MHz and 700 MHz spectrometers respectively. Spectra acquired on the 600 MHz spectrometer were collected with 4096×512 data points in the F2 and F1 dimensions respectively, while the spectra from the 700 MHz spectrometer had 4096×600 data points in these two dimensions. The spectral widths for the spectra from the 600 MHz and 700 MHz spectrometers were 8503.401 Hz and 8992.806 Hz respectively. Water suppression was achieved using excitation sculpting [45].

All spectra were processed using the NMRPipe software package [46]. The 2-D data were zero filled once in each dimension and Fourier transformed with a shifted sine-bell function. Spectral analysis was performed in NMRView version 5.2.2.01 [47] and chemical shifts were assigned according to well established methods [48].

Starting structures for the simulated annealing calculations were generated with CNS [49]. To generate the initial template structure of LFchimera, the topology files produced by CNS were manipulated to artificially insert the covalent amide link between the carbonyl C atom of Gly30 and the ζN atom of Lys280. Broad dihedral restraints were imposed on all of the non-Gly residues to keep the initial *phi* and *psi* angles within allowable regions of the Ramachandran plot. Peptide structures were calculated with ARIA 1.2 [50] using NOE restraints derived from the 2D ^{1}H-NOESY spectrum. Nine iterations of the simulated annealing protocol were performed with 20 structures generated in the first 7 iterations followed by 40 and 100 in the final two iterations. The 20 lowest energy structures from the final iteration were analyzed with Procheck [51] and visualized with MOLMOL [52].

3. Results

3.1. Differential scanning calorimetry

The influence of LFcin17–30, LFampB and LFchimera on the phase transitions of DPPG lipid suspensions is shown in Fig. 2. Pure DPPG lipids have a main phase transition peak at ~40 °C corresponding to the melting temperature (Tm) of the lipids converting from the gel phase to the liquid crystalline phase. In addition, a pretransition peak, corresponding to a conversion from the lamellar gel phase to the rippled gel phase, occurs at ~30 °C. At the lowest peptide:lipid ratio of 1:100, LFcin17–30 and LFampB had relatively mild effects on the phase transitions of the DPPG lipids. The Tm of the main phase transition and the pretransition is largely unaffected, as is the shape of these peaks. The LFchimera causes a broadening of the pretransition peak at this concentration, suggesting that this peptide interacts at the bilayer surface, however the main phase transition is also largely unaffected. As the concentration of peptide increases to a ratio of 1:10, all of the peptides cause substantial changes in the heating scans. LFcin17–30 has a sharp transition at ~40 °C as well as a broad transition centered at 43 °C. The higher temperature peak could be due to LFcin17–30 binding to the DPPG lipids, which rigidifies the bilayer and impedes the conversion to the liquid crystalline phase, while the lower temperature peak corresponds to DPPG lipids with no bound peptide. The effect of LFampB at high concentrations is opposite to LFcin17–30 with a broad transition appearing below the main phase transition and a sharp transition occurring at 38.9 °C. This suggests that LFampB destabilizes the gel phase and promotes the formation of the liquid crystalline phase. When the peptides were tested in combination with each other at the 1:10 ratio, the sharp main phase transition of unbound DPPG disappears and broad transitions at 38.7 °C and 43.7 °C emerge in the thermogram, consistent with the DPPG lipids interacting with LFcin17–30 and LFampB individually (Supplementary Figure S1).

The thermogram of LFchimera at a peptide:lipid ratio of 1:10 is unlike those described above and there appears to be a unique influence of the heterodimer on the phase behaviour of DPPG lipids. The main phase transition is broadened slightly with a sharp transition centred at a temperature of 40.3 °C, suggesting that the LFchimera impedes the formation of the liquid crystalline phase, similar to LFcin17–30. However, there is a low temperature shoulder to this main transition peak, which is similar to the broad shoulder seen in the thermogram of LFampB mixed with DPPG. Based on these observations, it is apparent that LFchimera has a strong effect on the phase transitions of DPPG lipids and that this effect is different from the constituent peptides or a mixture of the two.

3.2. Calcein leakage

LFcin17–30, LFampB or a mixture of the two peptides did not induce significant calcein leakage from either LUVs made from *E. coli* PLE or a 3:1 ratio of ePE:ePG (Fig. 3A and B). The lipid composition of *E. coli* PLE is 67% PE, 23% PG and 10% negatively charged cardiolipin (Avanti Polar Lipids Inc., avantipolarlipids.com), which is comparable to the negative charge present in the 3:1 ePE:ePG LUVs. Slightly higher leakage occurred when the peptides were added to LUVs composed of 1:1 ePE:ePG phospholipids (Fig. 3C). These LUVs have a greater net negative charge, due to the higher PG content, suggesting that electrostatic attractions with the cationic peptide contribute to the membrane disrupting ability of these two peptides. The addition of LFchimera to the LUVs resulted in significantly higher calcein release from all the negatively charged liposomes. For LUVs composed of *E. coli* PLE and 3:1 ePE:ePG, LFchimera induced 25% and 40% respectively at the highest peptide to lipid ratio. The membrane perturbing properties of LFchimera were also enhanced by increasing the negative charge on the LUV surface. Nearly 90% leakage was observed when LFchimera was added to vesicles composed of 1:1 ePE:ePG at a peptide:lipid ratio of 1:10. These results demonstrate that the LFchimera has enhanced membrane destabilizing activity compared to the constituent peptides.

3.3. Liposome fusion

Membrane fusion was examined by incubating ePE:ePG liposomes with increasing amounts of peptide and monitoring the change in absorbance of the solution at 400 nm [38,42]. The results from the liposome fusion assay are shown in Fig. 4. LFampB did not cause any vesicle fusion of negatively charged liposomes, while the addition of LFcin17–30 resulted in substantial increases in the absorbance values. The effect of adding LFchimera to the liposome suspensions was even more pronounced with a significant increase in absorbance at the lowest peptide:lipid ratio of 1:100 and absorbance values that were consistently higher than those observed for LFcin17–30 at equivalent peptide concentrations. The equimolar mixture of LFampB and LFcin17–30 caused liposome fusion that was practically identical to that seen for LFcin17–30 on its own (data not shown) suggesting that membrane fusion is a property of the LFcin peptide alone. These results demonstrate that LFcin17–30 induces fusion of negatively charged liposomes and that this fusion capacity is enhanced in the LFchimera peptide.

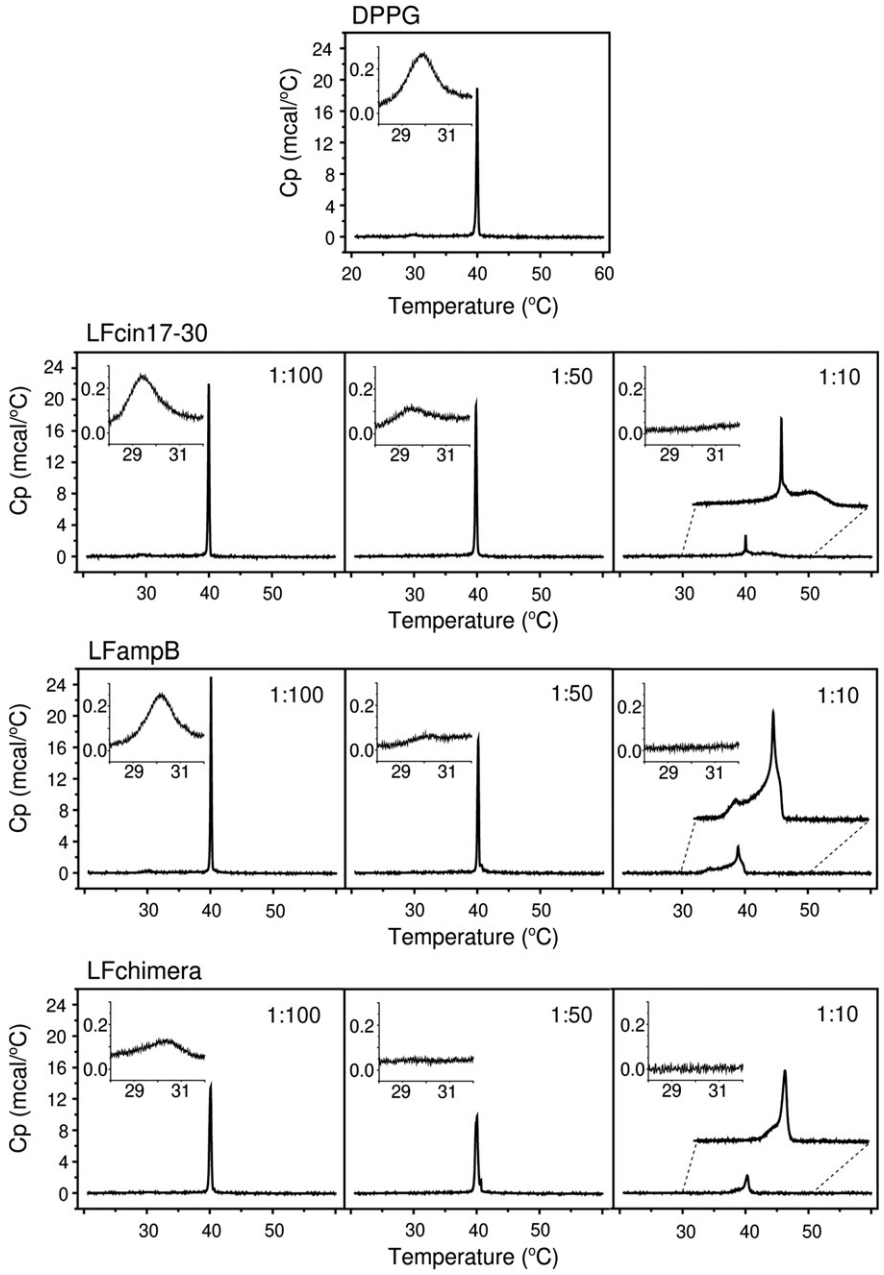

Fig. 2. DSC heating scans of pure DPPG compared to lipid suspensions containing LFcin17–30, LFampB and LFchimera at peptide to lipid molar ratios of 1:100, 1:50 and 1:10. The insets in each panel show the pretransition peak seen in the pure DPPG lipid sample. In addition, the main phase transition regions for each peptide sample at a ratio of 1:10 have been expanded to emphasize the features of the thermogram. All experiments were carried out at a lipid concentration of 1 mg/ml.

3.4. Circular dichroism spectroscopy

Structural analysis by CD spectroscopy provides a qualitative picture of the structural elements that are present in a given peptide solution. The ellipticity values measured by the spectropolarimeter are directly related to the number of amide bonds absorbing the circularly polarized light in the wavelength range. As expected, LFcin17–30 is the smallest peptide and has the smallest ellipticity intensity, while LFchimera is the largest molecule and has the greatest θ_{obs}. It should be noted that the spectrum collected for a sample containing 50 μM each of LFcin17–30 and LFampB was essentially identical to the curve obtained when the spectra of the individual peptides were added together (Supplementary Fig. S2). This is true for both the buffer and SDS samples and it suggests that the individual peptides do not physically interact with each other in solution and fold independently in the presence of detergent micelles.

Converting the ellipticity values to mean residue ellipticity corrects for the different molecular weights of the peptides and provides information about the secondary structure of the peptide. All peptides are largely unstructured in aqueous solution as indicated by the presence of a strong minimum peak at 200 nm (Fig. 5A). The intensity of the LFchimera peak at ~200 nm is larger than the other peptides possibly due to some structural conformation imposed on the hybrid peptide by the unique lysine linkage. In the presence of SDS micelles, negative peaks at 208 and 222 nm emerge in all the spectra, characteristic of peptides adopting helical conformations (Fig. 5B). For LFcin17–30, the intensities of the peaks at 208 and 222 nm are fairly weak. In fact, there is still a significant peak at ~205 nm, likely arising from peptide regions that remain unstructured in the presence of micelles. For LFampB and LFchimera, stronger minima are seen at 208 and 222 nm and the resulting spectra overlap almost identically with each other. This suggests that these two molecules have similar

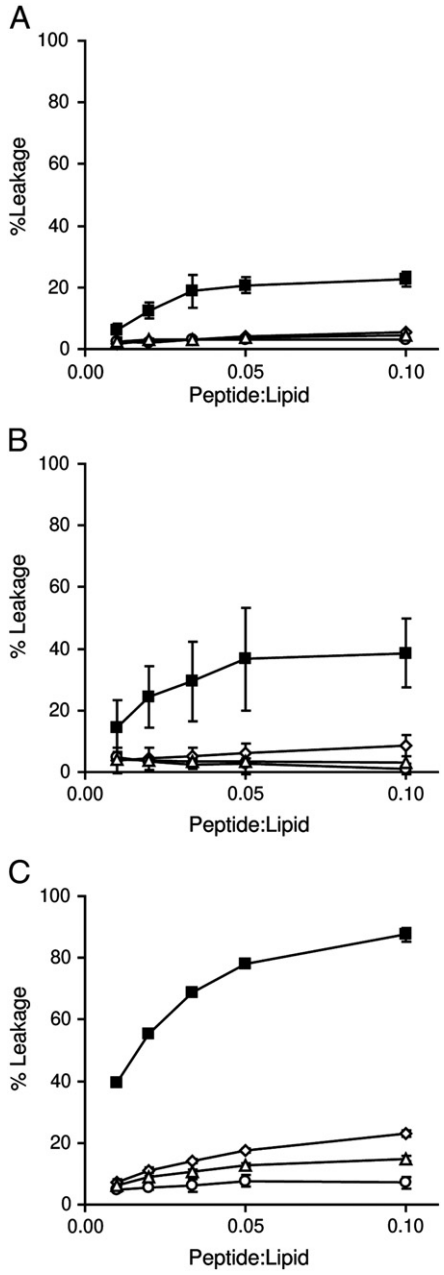

Fig. 3. Calcein leakage induced by LFampB (diamonds), LFcin17–30 (triangles), a mixture of the two peptides (circles), and LFchimera (filled boxes). The percentage of calcein dye released from LUVs composed of *E. coli* PLE (A), 3:1 ratio of ePE:ePG (B) and a 1:1 ratio of ePE:ePG (C) were measured. The error bars represent the standard deviation of three separate trials.

helical content; however, these helical conformations cannot be assigned to specific residues. The spectrum of LFampB mixed with LFcin17–30 represents an average of the secondary structure that is present and it is evident that the LFchimera possesses more helical conformation when bound to micelles than the mixture of the two peptides. Unfortunately, using only these results, it is unclear if the increased helical content of LFchimera is from the LFcin17–30 portion adopting a helical conformation or an extension of the N-terminal helix in LFampB, or a combination of both. Regardless, it is evident from the CD results that the linking lysine residue influences the micelle bound structure of the LFchimera peptide.

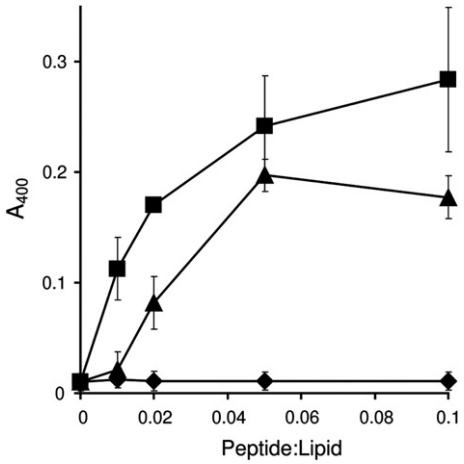

Fig. 4. Fusion of ePE:ePG liposomes induced by LFcin17–30 (triangles), LFampB (diamonds) and LFchimera (squares). An increase in the absorbance at 400 nm is indicative of liposome fusion. The error bars represent the standard deviation of three separate trials.

3.5. NMR results

Initially, we sought to determine the solution structure of the LFchimera bound to SDS micelles since this detergent is commonly used as a bacterial membrane mimic in NMR studies of antimicrobial peptides. In addition, the NMR solution structures of SDS bound

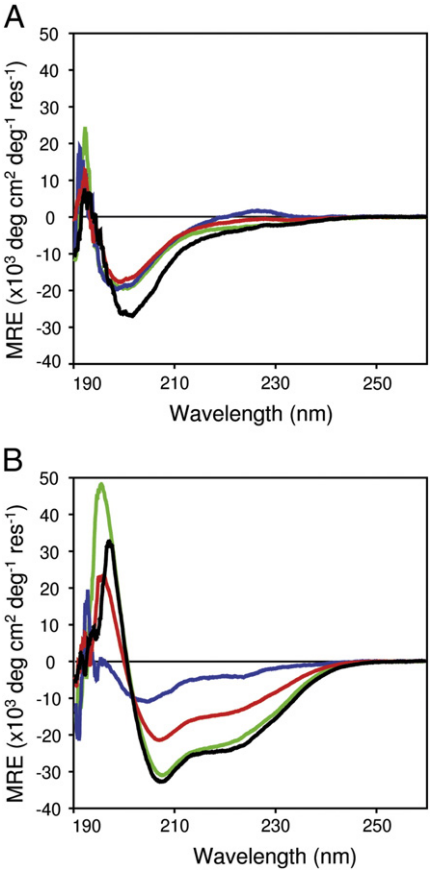

Fig. 5. Far UV CD spectra of LFampB (green), LFcin17–30 (blue), an equimolar mixture of the two peptides (red) and LFchimera (black). Data are shown in units of mean residue ellipticity (MRE). Spectra were acquired in buffer (A) and in the presence of 200 mM SDS (B). All spectra were recorded at room temperature at individual peptide concentrations of 50 μM.

LFampB [30, 31] and LFcin17–31 [23] have previously been solved by our group, which would allow for structural comparison among the peptides. Unfortunately, the 2D ^{1}H-NOESY spectrum of the LFchimera in the presence of SDS micelles had poor peak dispersion and the individual peaks could not be resolved (Supplementary Fig. S3). In an effort to improve the quality of the NMR spectra, a 4:4:1 mixture of chloroform, methanol and water was used as an alternative membrane mimetic. The resulting spectra were of much better quality with very well defined peaks and excellent peak dispersion making subsequent structure calculations possible (Supplementary Fig. S3).

NMR samples of LFcin17–30 and LFampB in the same co-solvent mixture were prepared to facilitate structural comparisons to LFchimera. Good peak dispersion was also observed for these two peptides allowing for complete chemical shift assignment of all protons (Fig. 6). It should be noted that the solution structure determination of LFampB was complicated by a large number of αH peaks between 4.1 and 4.3 ppm, resulting in significant peak overlap in this region. A similar phenomenon was seen in the spectrum of LFcin17–30 where several backbone amide chemical shifts appeared between 7.9 and 8.2 ppm, making unambiguous assignment of intermolecular NOEs in this region extremely difficult.

The solution structure of LFampB in the co-solvent mixture is shown in Fig. 6. A well defined N-terminal helix emerges in LFampB, while the cationic C-terminal region remains relatively unstructured. The backbone RMSD across the entire peptide is 1.552 Å but this drops to 0.919 Å across residues 265–278 (Fig. 7A). At first glance this appears to be a fairly large RMSD but this can be attributed to a lack of unambiguous NOEs between residues 272–277. The complication of the overlapping peaks between 4.1 and 4.3 ppm (described above) is compounded by the fact that all of the αH resonances between residues 272 and 277, inclusively, are found in this region of the spectrum. As a result, key medium range NOEs (dNN(i,$i+2$), dαN(i,$i+2$), dαN(i,$i+3$) and dαN(i,$i+4$)), that are important for defining helical structures, could not be unambiguously assigned for use in the structure calculations. If the backbone atoms of LFampB are fit across residues 265–272, whose medium-range NOEs were readily assigned, an extremely well defined helical conformation emerges with a backbone RMSD of 0.305 Å.

The side chain orientations of LFampB in the co-solvent are comparable to those seen in the SDS bound form of the peptide. The N-terminal helix is largely amphipathic with the hydrophobic residues appearing in a hydrophobic patch bordered by the aromatic side chains of Trp 268 and Phe 278 (Fig. 8). A number of charged residues appear on the opposite face of this hydrophobic patch, including three positively charged Lys residues at positions 269, 273 and 277 as well as a negative charge from Glu 276. The remaining cationic

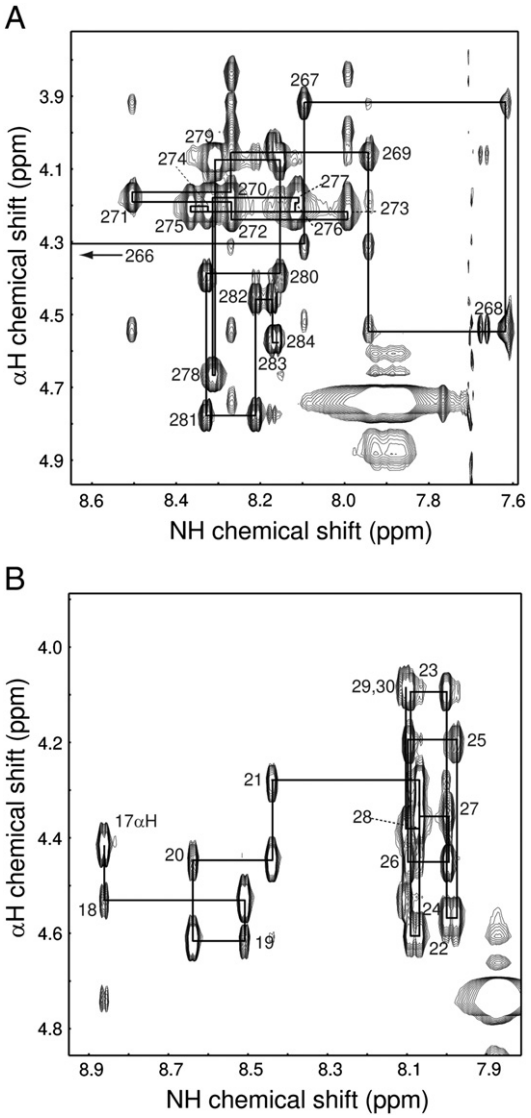

Fig. 6. NH–αH region of the 2D ^{1}H-NOESY spectra of LFampB (A) and LFcin17–30 (B) in a co-solvent mixture of chloroform, methanol and water collected on a 600 MHz spectrometer. All the chemical shifts for each peptide were assigned and the sequential connectivity between NH (i) and αH ($i-1$) peaks are indicated. Note the cluster of peaks that occurs between 4.1 and 4.3 ppm in the LFampB spectrum and the clustering of peaks between 7.9 and 8.2 ppm in the LFcin17–30 spectrum.

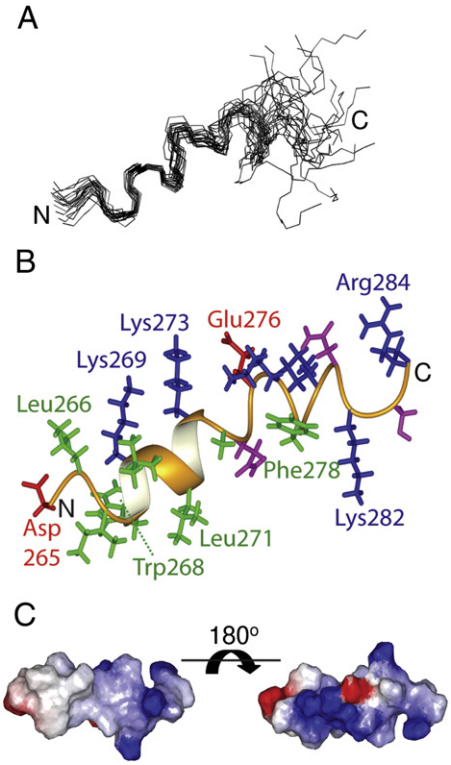

Fig. 7. Solution structure of LFampB in the co-solvent mixture. A relatively well defined N-terminal helix emerges when the backbones of the 20 lowest energy structures are superimposed across residues 265–278 (A). The ribbon diagram of a representative structure of LFampB shows the N-terminal helix and the orientation of the side chains in the peptide. Side chains are coloured as follows: hydrophobic — green, positively charged — blue, negatively charged — red and uncharged — magenta (B). The surface charge distribution of the peptide shows the amphipathic nature of the N-terminal helix (C). The panel on the left shows the peptide with the hydrophobic surface facing the reader and the panel on the right shows the charged surface on the opposite face of the structure.

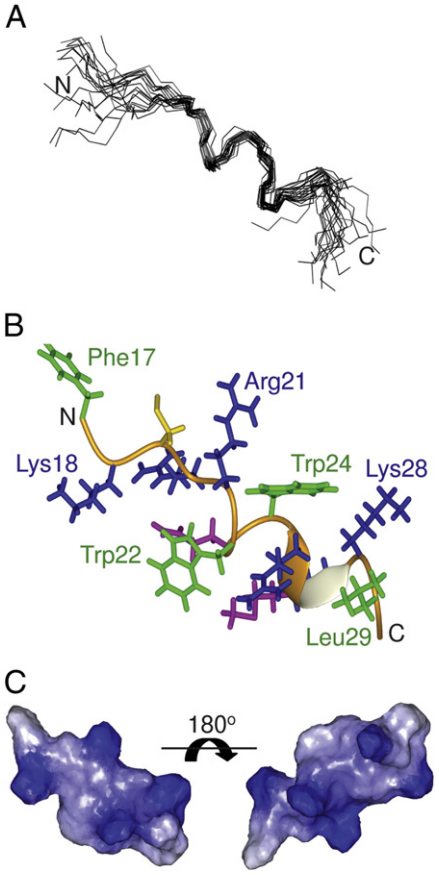

Fig. 8. Solution structure of LFcin17–30 in a 4:4:1 mixture of chloroform, methanol and water. The peptide adopts a short helical conformation between residues 20–28, with a backbone RMSD of 0.503 Å (A). The ribbon diagram of a representative structure of LFcin17–30 clearly shows this short helical segment. The side chain orientations are also shown and have been colored using the same scheme described in Fig. **6**. In addition, the cysteine residue is shown in yellow (B). The surface charge distribution of the peptide does not show a distinct amphipathic structure (C). The panel on the left shows the peptide in the same orientation as in B and the panel on the right shows the opposite face.

residues are found in the C-terminal region, which is disordered compared to the rest of the peptide.

The structure of LFcin17–30 in the co-solvent mixture is also not very well defined across the length of the peptide, as indicated by a large backbone RMSD of 1.327 Å across all residues. However, if the backbone atoms of the 20 lowest energy structures are overlaid between Arg 20 and Lys 28, the RMSD drops to 0.503 Å, corresponding to a small helix-like conformation (Fig. 9). Contrary to the LFampB structure, the solution structure of LFcin17–30 in the co-solvent is not very amphipathic. The two Trp residues at positions 22 and 24 appear on the same face of the peptide, forming a small hydrophobic region, but the cationic Lys and Arg residues are fairly evenly distributed across the surface of the molecule.

The structure of the LFchimera in the membrane mimetic solvent is interesting because it is the first high resolution structure reported for a molecule containing this unique lysine linkage. The lysine linkage between LFcin17–30 and LFampB keeps the C-termini of these two peptides in close proximity to each other as would be observed if they were excised directly from the crystal structure of bovine lactoferrin [18]. The solution structure of the LFchimera presented here indicates that the linker does not maintain the orientation of LFcin17–30 relative to LFampB compared to these stretches in intact lactoferrin. However, the lysine linker does induce structural changes in the LFampB and LFcin17–30 portions of LFchimera compared to the conformations of the individual peptides on their own.

The NOESY spectrum of LFchimera collected on the 700 MHz spectrometer yielded sharper peaks and better dispersion compared to the spectra collected at a lower magnetic field strength. This alleviated some of the peak overlap that was seen in the LFampB and LFcin17–30 spectra, which would have made solving the structure of such a large antimicrobial peptide using only proton NMR techniques virtually impossible. All of the chemical shifts of the protons in the LFchimera peptide were assigned based on the NOESY spectrum and the backbone connectivity was easily determined. In addition, the presence of the peptide bond between the C-terminus of LFampB and the amide on the side chain of the linking lysine residue was confirmed through the identification of cross peaks in the NOESY spectrum (Fig. 9).

Initial analysis of the LFchimera structure revealed a backbone RMSD of 4.278 Å when the 20 lowest energy structures were fit across all residues. This could suggest that this peptide does not adopt a well defined overall conformation in the co-solvent mixture. There are only a handful of NOEs between the LFampB and LFcin17–30 portions of LFchimera and most of these are limited to interactions between the side chain of Arg 284 and the side chain protons of the Lys linker. No NOEs were observed between the two peptides further away from the connecting lysine residue resulting in a large degree of relative conformational freedom between the two polypeptide chains. However, a closer inspection of the LFchimera structure in the co-solvent mixture reveals that the LFampB and LFcin17–30 portions of LFchimera fold independently from each other under these conditions.

Analysis of the LFampB and LFcin17–30 portions of LFchimera reveals well defined backbone conformations for each constituent polypeptide in the heterodimer. The backbone RMSD of all the LFampB residues in LFchimera is 0.933 Å (Fig. 10A, right) which corresponds to a fairly well defined helical conformation that extends into the normally flexible cationic C-terminal region of LFampB (see Fig. 7). The backbone RMSD of all the LFcin17–30 residues in LFchimera is 2.212 Å but the structure converges to a well defined conformation between Arg 20 and Gly30 as seen by a comparatively low backbone RMSD of 0.746 Å across these eleven residues (Fig. 10A, left). This is a comparable RMSD to that calculated for a similar region of free LFcin17–30 (see above) but it includes two extra residues indicating that, in the co-solvent, this portion of the LFcin17–30 peptide is more ordered in the LFchimera heterodimer.

Knowing the structure of LFampB, LFcin17–30 and LFchimera in the co-solvent solution provides an opportunity to compare between the structures and examine the structural differences induced by the presence of the linking lysine residue. If we compare the TOCSY spectra of the three molecules, a number of the peaks from LFcin17–30 and LFampB overlap with the peaks of the LFchimera (Supplementary Fig. S4A). The peaks that are shifted represent residues that have a different conformation in the LFchimera structure. As expected, the peaks that are significantly shifted in the LFchimera TOCSY spectrum correspond to residues that are close to the linking lysine residue (Supplementary Fig. S4B). This underscores the structural impact of the Lys linker on the conformation of the hybrid peptide.

A representative structure of the LFchimera in the co-solvent is shown in Fig. 10B. The LFampB portion forms a nearly contiguous helix across the length of the peptide, including a number of residues in the cationic C-terminal region. The increased helical content in LFcin17–30 is even more pronounced with a fairly well defined helical conformation observed between Arg20 and Gly30. Overall, this represents an ordering of the C-terminal regions of both peptides when they are joined together in the LFchimera heterodimer.

The secondary structure of LFchimera in the miscible co-solvent supports the CD results, which indicated that the hybrid peptide adopted a mainly α-helical conformation when bound to SDS micelles. Based on what is known about the solution structure of LFampB, there are a number of residues in the C-terminal region

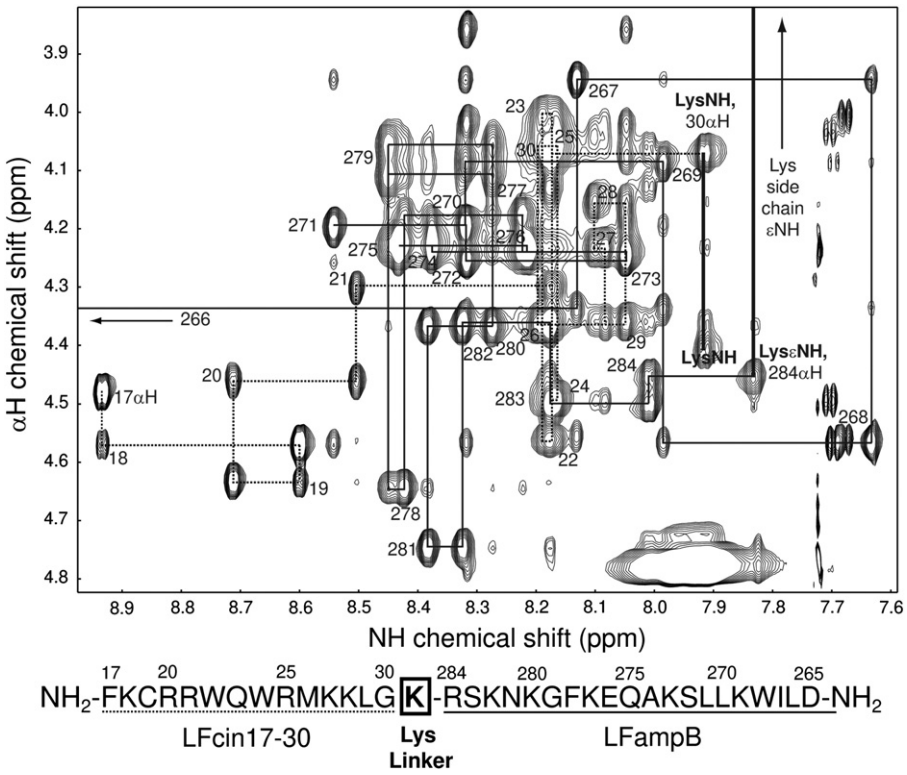

Fig. 9. Sequence specific assignment for the LFchimera based on 2D ^{1}H-NOESY spectrum collected on a 700 MHz spectrometer. The sequence of LFchimera is also shown and has been highlighted according to the labelled peaks in the NOESY spectrum. NOE cross peaks to the linking lysine residue are also indicated.

that do not readily form a helix. An examination of the LFchimera structure reveals a number of residues that also do not form helices, but these are found mostly in the N-terminal region of the LFcin17–30 portion. This explains why the CD spectra of LFampB and LFchimera overlap with each other (Fig. 3B) since both polypeptides contain helical regions with a small fraction of residues adopting random coil conformations.

A survey of the surface charge distribution in LFchimera indicates that the peptide does not adopt an amphipathic structure over the entire surface of the peptide. The amphipathic helix in LFampB persists in the LFchimera structure, while the LFcin17–30 region still does not show a clear separation of charged and hydrophobic residues (Fig. 10C).

Structural statistics for the solution structures of LFampB, LFcin17–30 and LFchimera in the co-solvent mixture are shown in Table 1. It should be noted that the residues that occupy the disallowed regions of the Ramachandran plot in LFchimera are found in the flexible N-terminal region of the LFcin17–30 polypeptide. Therefore, these disallowed dihedral angles can be attributed to a large degree of conformational flexibility in the peptide as opposed to a significant structural feature of the peptide backbone.

4. Discussion

Antimicrobial peptides are seldom found in isolation in nature. Many peptides are biosynthetically produced in combination with a variety of others, yielding a potent cocktail of antibiotic molecules capable of challenging a range of pathogenic micro-organisms that threaten the host. Many animals employ mixtures of antimicrobial peptides as important components of their innate immune systems. For instance, amphibians secrete a number of antimicrobial peptides and frog skin has proven to be a wealthy source of potent antimicrobial sequences [53–59]. In insects, antimicrobial peptides make up a significant portion of their innate immune response [60, 61]. Cows generate at least 38 antimicrobial peptides which differ significantly in their sequences and respective structures [62]. Even humans produce an array of antimicrobial peptides including ubiquicidin, LL-37, HBD1–3 and HNP1, among others [63].

Since antimicrobial peptides often act in combination, joining different sequences may be an effective strategy to develop novel antibiotics with enhanced antimicrobial potency. Numerous studies have examined the antimicrobial activity of peptide sequences joined together in one continuous polypeptide chain. For example, several studies have focused on hybrid peptides which combine portions of Cecropin A and melittin [64–68]. A similar strategy has been used to generate a series of hybrid peptides between Cecropin B and thanatin, one of which exhibited moderate antifungal activity not seen in either of the parent peptides [69].

Some antimicrobial peptides exist in dimeric form when bound to vesicles, such as magainin 2 [70] and its derivative, MSI-78 [71]. This observation has led to the generation of covalently linked peptide dimers, typically through the incorporation of cysteine residues into the peptide sequences followed by oxidation to generate a disulphide linked dimer. This strategy has been successfully used to generate parallel and antiparallel dimers of magainin 2 [72] and dimeric forms of lentivirus-derived antimicrobial peptides [73]. In both cases, peptide dimerization resulted in hybrid peptides with enhanced antimicrobial activity.

The lysine linkage used in the LFchimera molecule has also been used to join antimicrobial peptides together; however, the effectiveness of Lys dimerization on the biological properties of peptides is unpredictable. For instance, a lysine branched dimer of a *de novo* decapeptide was found to have potent activity against *E. coli* and *S. aureus* while being relatively non-cytotoxic and resistant to proteases [74]. In contrast, the dimerzation of a tritrpticin derived peptide, PST13-RK, through both Cys- and Lys-linkages yielded a dimeric peptide with modestly higher antibacterial activity accompanied by an undesired increase in toxicity towards mammalian cells [75].

One of the best examined examples of a linked heterodimer of two antimicrobial peptides is that between two frog peptides, magainin2

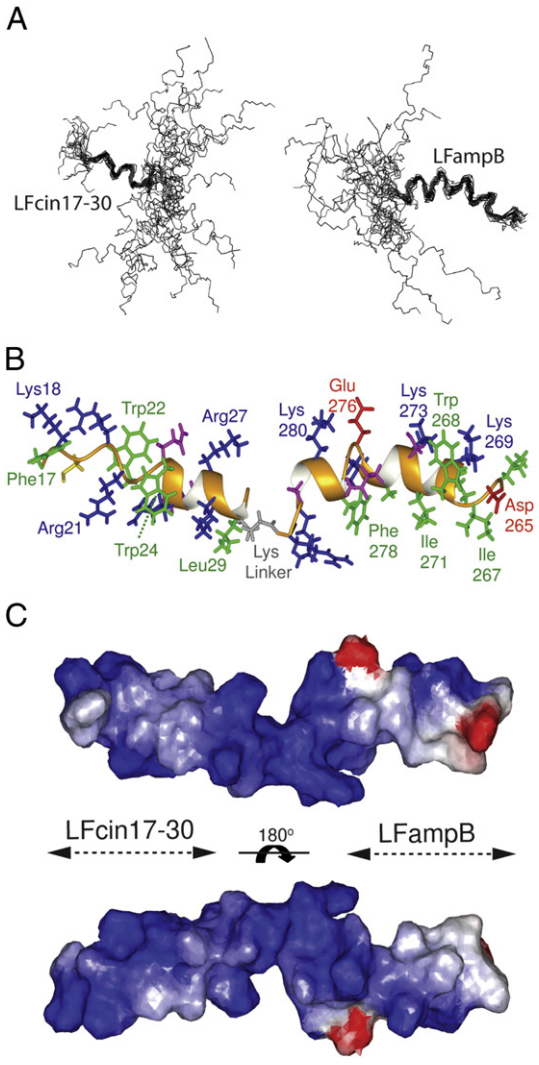

Fig. 10. Overlay of all the backbone atoms of the 20 lowest energy structures of LFchimera in the co-solvent mixture of chloroform:methanol:water (A). The superposition of the backbone atoms corresponding to the residues of LFampB reveals a well defined helical conformation with a backbone RMSD of 0.933 Å (A, right). When the backbone atoms are overlaid across residues 20–30 of LFcin17–30, the RMSD is 0.746 Å (A, left). The ribbon diagram of a representative structure of the LFchimera in the co-solvent mixture shows significant helical conformation (B). Residues have been coloured using the same scheme seen in previous figures. The linking lysine residue connecting LFampB and LFcin17–30 is shown in grey. The surface charge distribution of LFchimera reveals no overall amphipathicity in the heterodimer (C). The LFchimera molecule is shown in the same orientation as in B and rotated along the X-axis to show the opposite face. Cationic surfaces are coloured in blue, anionic regions are shown in red and uncharged portions are white.

and PGLa. Both of these peptides are secreted by the epithelial cells of the African clawed frog, *Xenopus laevis* [59, 76], and individually they posses broad spectrum antimicrobial activity against a variety of bacterial species. When tested in combination, magainin 2 and PGLa demonstrated marked synergism, both in their antimicrobial activities and in their membrane destabilizing properties [77, 78]. This observation led to the synthesis of a hybrid peptide where both peptides were linked together through a disulphide bond [6]. This hybrid peptide displayed similar activity compared to the mixture of the two peptides and the solution structure of this hybrid peptide bound to DPC micelles demonstrated that the two helices are partially held together by a series of interstrand NOEs between magainin 2 and PGLa [7].

Many of the studies on dimerized antimicrobial peptides, through either Cys- or Lys-linkages, have limited their structural analysis to CD spectroscopy to look at the overall conformational changes that occur upon lipid binding. The NMR structure of LFchimera presented here represents the first high-resolution structure of a peptide containing this unique Lys-linkage and it is a significant contribution towards furthering our understanding of the mode of action of this class of linked antimicrobial peptides. Structural characterization of LFampB, LFcin17–30 and LFchimera has previously been performed using CD spectroscopy [33]. All of the peptides were unstructured in aqueous buffer, consistent with the CD results presented here, but when mixed with DMPG liposomes; each of the peptides underwent a conformational change. In agreement with our results, LFcin17–30 changed conformation but it did not form a strong α-helix, while LFampB mixed with the anionic liposomes yielded CD spectra characteristic of α-helical structure. The CD spectrum of LFchimera mixed with DMPG also appeared to be largely helical, but the intensity of the peaks at 208 and 222 nm were largely reduced compared to LFampB. This could be due to aggregation of the peptide with the DMPG liposomes, as seen in the fusion assay with ePE:ePG liposomes (Fig. 4), which would result in a loss of CD signal. Full length bovine LFcin has the ability to induce fusion of negatively charged liposomes [38] and it is evident that this is a trait that is retained in LFcin17–30 and LFchimera. Regardless, the increased helical content in the LFchimera upon membrane binding seen in the CD results is likely an important structural feature afforded to this molecule by the linking lysine residue.

A brief discussion regarding the choice of the NMR solvent used in this study is warranted owing to the inherent differences between aqueous samples containing detergent micelles and co-solvent mixtures containing organic solvents. Typically, NMR structural studies of antimicrobial peptides are carried out in the presence of deuterated detergent micelles [79]. Unfortunately, the spectrum of an NMR sample containing the LFchimera and SDS was of such poor quality that further structural characterization was not possible. The poor spectral resolution might be explained if we assume that the LFampB and LFcin17–30 regions of LFchimera bind to separate SDS micelles. Binding of each peptide region to individual micelles would lead to larger LFchimera/micelle aggregates that tumble slowly in solution and could explain the broad peptide signals seen in the NOESY spectrum (Supplementary Fig. S3). Indeed, we did observe evidence for membrane fusion in our liposome aggregation studies.

The co-solvent mixture of 4:4:1 chloroform, methanol and water is considered to be a reasonable mimic of the membrane environment. Many functional properties of membrane associated proteins are conserved when they are dissolved in this single phase mixture [80, 81]. Additionally, a variety of NMR structural studies of transmembrane proteins have been published using this co-solvent mixture [80, 82, 83] and our group has used this mixture to examine the solution structures of membrane associated antimicrobial peptides [15, 44].

The most compelling evidence that the co-solvent mixture yields an accurate representation of the solution structure of an antimicrobial peptide bound to a membrane involves comparing the SDS bound structures of LFcin17–30 and LFampB to the structures determined in the co-solvent mixture. The structure of LFampB in the co-solvent mixture is remarkably similar to the SDS bound conformation of the peptide [31]. The characteristic flexibility seen in the C-terminal region and the amphipathic N-terminal helix is present in both structures. There may be a slight increase in the helical content of the co-solvent derived structure but this can be attributed to the promotion of helical conformation in peptides by organic solvents, as is the case with 2,2,2-trifluoroethanol [84, 85].

The NMR solution structure of LFcin17–31 bound to SDS micelles has previously been reported [23] and compared to our LFcin sequence, this peptide has an additional Ala residue at the C-terminus and the C-terminal carboxyl group is amidated. The SDS bound LFcin17–31 peptide does not adopt a helical conformation and

Table 1
Structural statistics for the ARIA generated structures of LFampB, LFcin17–30 and LFchimera in a co-solvent mixture of choloroform, methanol and water.

	LFampB	LFcin17–30	LFchimera
No. of distance restraints			
Unambiguous NOEs	272	208	605
Ambiguous NOEs	15	13	41
Unassigned NOEs	0	0	0
Total NOEs	287	221	646
Dihedral restraints	18	12	31
Geometry analysis — root mean square			
Bonds (Å)	$1.48\times10^{-3}+/-4.0\times10^{-5}$	$8.17\times10^{-4}+/-1.2\times10^{-4}$	$2.09\times10^{-3}+/-5.0\times10^{-5}$
Angles (degree)	$0.302+/-1.8\times10^{-3}$	$0.284+/-2.6\times10^{-3}$	$0.343+/-5.8\times10^{-3}$
Impropers (degree)	$0.117+/-6.7\times10^{-3}$	$0.103+/-8.7\times10^{-3}$	$0.163+/-1.6\times10^{-2}$
Dihedrals (degree)	37.81 +/− 0.37	37.44 +/− 0.78	9.18 +/− 0.37
van der Waals (kcal/mol)	5.76 +/− 0.27	3.29 +/− 0.15	46.75 +/− 1.99
Ramachandran space (%)[a]			
Most favoured	78.8	56.7	66.7
Additionally allowed	21.2	43.4	29.1
Generously allowed	0.0	0.0	2.9
Disallowed	0.0	0.0	1.2

[a] Calculated by Procheck [51].

instead forms a well defined turn like structure. Interestingly, the structure of LFcin17–31 is moderately amphipathic in contrast to the structure of LFcin17–30 determined in the co-solvent mixture. It seems that the co-solvent mixture induces slightly more helical conformation in the LFcin17–30 backbone, which alters the orientation of the Arg and Lys residues on the surface of the peptide and makes it difficult to identify a continuous hydrophobic face. However, the two Trp residues at positions 22 and 24 do appear on the same side of the LFcin17–30 structure. This small hydrophobic face formed by these two Trp residues is similar to a portion of the hydrophobic surface seen in the SDS bound LFcin17–31 peptide. Trp residues are known to have a preference for the interfacial region of a bilayer [86, 87] and recent molecular dynamics simulations of bovine LFcin performed in 4:4:1 chloroform–methanol–water suggests that these two Trp residues anchor the peptide to the surface of the bacterial membrane [88]. This offers further support that the LFcin17–30 structure determined in this study is representative of the peptide conformation bound to a bilayer.

Based on these observations, we can conclude that the solution structure of LFchimera is a reasonable representation of the structure of the peptide bound to a bacterial membrane. However, contrary to the solution structure of the magainin2-PGLa heterodimer discussed earlier [7], interstrand NOEs between the LFampB and LFcin17–30 portions of LFchimera were not observed in the 2D NOESY spectrum. This suggests that the increased antimicrobial activity of the LFchimera is not related to a combined structural component involving both peptides. Instead, it is likely related to a combination of the mechanisms of action of LFcin17–30 and LFampB, which are enhanced in the LFchimera peptide.

The membrane destabilizing activity seen in the calcein leakage results is difficult to ascribe to either the LFampB or the LFcin17–30 region of the LFchimera. Both peptides had significant effects on the thermotropic phase behaviour of DPPG lipid suspensions but neither peptide caused significant leakage from calcein encapsulated LUVs. Full length bovine LFcin has been shown to induce leakage from negatively charged liposomes [38], but the extent of membrane disruption appears to depend on the nature of the acyl chain [89]. Conversely, calcein leakage experiments conducted with bovine LFcin fragments have demonstrated that they cause poor leakage from all types of vesicles, regardless of acyl chain composition [19, 23]. For lactoferrampin, this is the first time that calcein leakage has been reported for this peptide, but it is known that LFampB preferentially interacts with anionic phospholipids [30, 31] and recent evidence suggests that this peptide can induce a micellar cubic phase in DMPC/DMPG liposomes [90]. Previously published DSC results for LFcin17–30 and LFampB mixed with DMPG liposomes revealed that these peptides influenced lipid organization at relatively high peptide concentrations, while the LFchimera caused more dramatic changes to the phase transition of DMPG liposomes at lower peptide concentrations [33]. This is in agreement with the DSC results presented here wherein the pretransition peak of DPPG is significantly affected in the LFchimera sample at a lipid:peptide ratio of 1:100 while the pretransition peak is largely intact in the presence of LFcin17–30 or LFampB at the same concentration. A number of studies have examined the effects of these peptides on intact bacterial cells. Atomic force microscopy of *E. coli* and *S. aureus* treated with bovine LFcin revealed that the peptide had significant effects on the bacterial membrane structure without disrupting the overall membrane integrity [20]. Freeze-fracture transmission electron microscopy studies of LFampB and LFcin17–30 demonstrated that both peptides have dramatic effects on the plasma membrane integrity of *C. albicans* and *E. coli* [29] and severe membrane damage was observed when LFchimera was added to *V. parahaemolyticus* [34]. Evidently, the LFchimera heterodimer significantly destabilizes lipid bilayers, which likely explains some of the increased activity of the hybrid peptide.

The increase in membrane permeability induced by the LFchimera is correlated with an increased positive charge of the LFchimera compared to the individual peptides. The net positive charges of LFampB and LFcin17–30 are +4 and +6 respectively. When combined in the LFchimera peptide, the net charge becomes +12 (the LFampB carboxyl group is in a peptide bond with the ε-amino group on the Lys linker and the α-carboxyl group on the Lys linker is amidated, effectively removing two negative charges) which should result in a stronger electrostatic attraction to the negatively charged surface of bacterial cells. This is consistent with the increased leakage observed from LUVs with higher negative charge on their surface, as the electrostatic attraction is stronger towards the highly cationic LFchimera molecule. How this increased cationic nature of LFchimera leads to increased membrane permeability is still unclear but we can speculate based on the mechanism of action proposed for LFampB. Binding of LFampB to the microbial surface involves an initial electrostatic attraction between the cationic residues in the C-terminal region of the peptide followed by folding and insertion of the N-terminal amphipathic helix into the interfacial region of the phospholipid bilayer [30–32]. This electrostatic attraction is a critical interaction for the mode of action of LFampB, since adding positive charges to the C-terminal region of human lactoferrampin has been shown to increase the antimicrobial activity of this peptide [32]. The addition of LFcin17–30 to the C-terminus of LFampB adds six cationic residues to the normally flexible C-terminal portion of LFampB. This increased positive charge in LFchimera might drive the hybrid peptide to the bacterial membrane which promotes the formation of the N-

terminal helix in the LFampB portion of the peptide and, in turn, increases the membrane perturbing activity of the peptide. An extension of the increased positive charge when LFcin17–30 and LFampB are joined together is that this also increases the hydrophobic bulk in the heterodimer, which would presumably favour interactions between the peptide and the hydrophobic core of a membrane.

Determining the solution structure of micelle bound antimicrobial peptides continues to be of interest to researchers in the field as evidenced by recent high resolution NMR structures reported for micelle bound LL-37 [91], lactophoricin [92], and papiliocin [93]. However, the limitations of using micellar and membrane mimetics in NMR spectroscopy are well known. There is significant positive curvature at the surface of a micelle which can influence the structure of a peptide. Miscible co-solvents alleviate the curvature problem and can help improve spectral resolution. However, interactions between the peptide and lipid head groups or acyl chains cannot be determined using this method. Therefore, based on the NMR structure of the LFchimera in the co-solvent mixture, we can only speculate as to how this hybrid peptide disrupts phospholipid bilayers at the molecular level. Future studies could involve the use of bicelles [94] or solid state NMR with lipid and peptide mixtures [95], both of which could provide significant insights into the conformation and orientation of the peptide in a bilayer. Furthermore, molecular dynamics studies [96] could be used to examine the conformation of LFchimera as it interacts with membranes.

Finally, in addition to causing membrane perturbations, it is possible that LFchimera has an intracellular target for antimicrobial activity. In an attempt to explain the apparent weak membrane activity of bovine LFcin, it has been suggested that this peptide crosses the bacterial membrane and binds to intracellular targets [19, 23, 97]. Indeed, bovine LFcin localizes to the cytoplasm of bacterial cells [98] and has been shown to inhibit macromolecular synthesis of DNA, RNA and proteins in *E. coli* and *B. subtilis* [99]. The increased antimicrobial activity of the LFchimera could therefore be attributed to combined effect of the increased ability to disrupt bacterial membranes which, in turn, provides entry into the cell and increases access to intracellular targets. Collectively, these two modes of action would lead to a substantial increase in the antimicrobial potency of the LFchimera compared to either LFampB or LFcin17–30 on their own.

Supplementary materials related to this article can be found online at doi:10.1016/j.bbamem.2011.11.023

Acknowledgements

The authors would like to thank Dr. Deane McIntyre for technical assistance and maintenance of the Bio-NMR facility at the University of Calgary. The authors are grateful to Dr. Leonard T. Nguyen for preparing the template LFchimera structure files and modifying the peptide topology files used in the structure calculations. JGMB and KN are supported by a grant from the University of Amsterdam for research into the focal point of "Oral Infections and Inflammation". HJV holds a Scientist award from the Alberta Heritage Foundation for Medical Research. This work is supported by a grant from the Canadian Institutes of Health Research program for "Novel Alternatives to Antibiotics".

References

[1] L.T. Nguyen, E.F. Haney, H.J. Vogel, The expanding scope of antimicrobial peptide structures and their modes of action, Trends Biotechnol. 29 (2011) 464–472.
[2] H. Yan, R.E.W. Hancock, Synergistic interactions between mammalian antimicrobial defense peptides, Antimicrob. Agents Chemother. 45 (2001) 1558–1560.
[3] A. Romanelli, L. Moggio, R.C. Montella, P. Campiglia, M. Iannaccone, F. Capuano, C. Pedone, R. Capparelli, Peptides from Royal Jelly: studies on the antimicrobial activity of jelleins, jelleins analogs and synergy with temporins, J. Pept. Sci. 17 (2011) 348–352.
[4] K. Matsuzaki, Y. Mitani, K. Akada, O. Murase, S. Yoneyama, M. Zasloff, K. Miyajima, Mechanism of synergism between antimicrobial peptides magainin 2 and PGLa, Biochemistry 37 (1998) 15144–15153.
[5] M. Cassone, L. Otvos Jr., Synergy among antibacterial peptides and between peptides and small-molecule antibiotics, Expert Rev. Anti-Infect. Ther. 8 (2010) 703–716.
[6] M. Nishida, Y. Imura, M. Yamamoto, S. Kobayashi, Y. Yano, K. Matsuzaki, Interaction of a magainin-PGLa hybrid peptide with membranes: insight into the mechanism of synergism, Biochemistry 46 (2007) 14284–14290.
[7] E.F. Haney, H.N. Hunter, K. Matsuzaki, H.J. Vogel, Solution NMR studies of amphibian antimicrobial peptides: linking structure to function? Biochim. Biophys. Acta 1788 (2009) 1639–1655.
[8] B.C. Chu, A. Garcia-Herrero, T.H. Johanson, K.D. Krewulak, C.K. Lau, R.S. Peacock, Z. Slavinskaya, H.J. Vogel, Siderophore uptake in bacteria and the battle for iron with the host; a bird's eye view, Biometals 23 (2010) 601–611.
[9] P.K. Singh, M.R. Parsek, E.P. Greenberg, M.J. Welsh, A component of innate immunity prevents bacterial biofilm development, Nature 417 (2002) 552–555.
[10] L. Adlerova, A. Bartoskova, M. Faldyna, Lactoferrin: a review, Vet. Med. 53 (2008) 457–468.
[11] S.A. Gonzalez-Chavez, S. Arevalo-Gallegos, Q. Rascon-Cruz, Lactoferrin: structure, function and applications, Int. J. Antimicrob. Agents 33 (2009) 301–308.
[12] D. Legrand, J. Mazurier, A critical review of the roles of host lactoferrin in immunity, Biometals 23 (2010) 365–376.
[13] M. Tomita, W. Bellamy, M. Takase, K. Yamauchi, H. Wakabayashi, K. Kawase, Potent antibacterial peptides generated by pepsin digestion of bovine lactoferrin, J. Dairy Sci. 74 (1991) 4137–4142.
[14] W. Bellamy, M. Takase, K. Yamauchi, H. Wakabayashi, K. Kawase, M. Tomita, Identification of the bactericidal domain of lactoferrin, Biochim. Biophys. Acta 1121 (1992) 130–136.
[15] H.N. Hunter, A.R. Demcoe, H. Jenssen, T.J. Gutteberg, H.J. Vogel, Human lactoferricin is partially folded in aqueous solution and is better stabilized in a membrane mimetic solvent, Antimicrob. Agents Chemother. 49 (2005) 3387–3395.
[16] J.L. Gifford, H.N. Hunter, H.J. Vogel, Lactoferricin: a lactoferrin-derived peptide with antimicrobial, antiviral, antitumor and immunological properties, Cell. Mol. Life Sci. 62 (2005) 2588–2598.
[17] P.M. Hwang, N. Zhou, X. Shan, C.H. Arrowsmith, H.J. Vogel, Three-dimensional solution structure of lactoferricin B, an antimicrobial peptide derived from bovine lactoferrin, Biochemistry 37 (1998) 4288–4298.
[18] S.A. Moore, B.F. Anderson, C.R. Groom, M. Haridas, E.N. Baker, Three-dimensional structure of diferric bovine lactoferrin at 2.8 angstrom resolution, J. Mol. Biol. 274 (1997) 222–236.
[19] L.T. Nguyen, D.J. Schibli, H.J. Vogel, Structural studies and model membrane interactions of two peptides derived from bovine lactoferricin, J. Pept. Sci. 11 (2005) 379–389.
[20] Y. Liu, F. Han, Y. Xie, Y. Wang, Comparative antimicrobial activity and mechanism of action of bovine lactoferricin-derived synthetic peptides, Biometals 24 (2011) 1069–1078.
[21] L.T. Nguyen, J.K. Chau, N.A. Perry, L. de Boer, S.A. Zaat, H.J. Vogel, Serum stabilities of short tryptophan- and arginine-rich antimicrobial peptide analogs, PLoS One 5 (2010) e12684.
[22] D.J. Schibli, P.M. Hwang, H.J. Vogel, The structure of the antimicrobial active center of lactoferricin B bound to sodium dodecyl sulfate micelles, FEBS Lett. 446 (1999) 213–217.
[23] W. Jing, J.S. Svendsen, H.J. Vogel, Comparison of NMR structures and model-membrane interactions of 15-residue antimicrobial peptides derived from bovine lactoferricin, Biochem. Cell Biol. 84 (2006) 312–326.
[24] M.I.A. van der Kraan, J. Groenink, K. Nazmi, E.C.I. Veerman, J.G.M. Bolscher, A.V.N. Amerongen, Lactoferrampin: a novel antimicrobial peptide in the N1-domain of bovine lactoferrin, Peptides 25 (2004) 177–183.
[25] M.I.A. van der Kraan, K. Nazmi, W. van't Hof, A.V.N. Amerongen, E.C.I. Veerman, J.G.M. Bolscher, Distinct bactericidal activities of bovine lactoferrin peptides LFampin 268–284 and LFampin 265–284: Asp-Leu-Ile makes a difference, Biochem. Cell Biol. 84 (2006) 358–362.
[26] M.I.A. van der Kraan, C. van der Made, K. Nazmi, W. van't Hof, J. Groenink, E.C.I. Veerman, J.G.M. Bolscher, A.V.N. Amerongen, Effect of amino acid substitutions on the candidacidal activity of LFampin 265–284, Peptides 26 (2005) 2093–2097.
[27] M.I.A. van der Kraan, K. Nazmi, A. Teeken, J. Groenink, W. t Hof, E.C.I. Veerman, J.G.M. Bolscher, A.V.N. Amerongen, Lactoferrampin, an antimicrobial peptide of bovine lactoferrin, exerts its candidacidal activity by a cluster of positively charged residues at the C-terminus in combination with a helix-facilitating N-terminal part, Biol. Chem. 386 (2005) 137–142.
[28] R. Adao, K. Nazmi, J.G. Bolscher, M. Bastos, C- and N-truncated antimicrobial peptides from LFampin, J. Pharm. Bioallied. Sci. 3 (2011) 60–69.
[29] M.I.A. van der Kraan, J. van Marle, K. Nazmi, J. Groenink, W. van't Hof, E.C.I. Veerman, J.G.M. Bolscher, A.V.N. Amerongen, Ultrastructural effects of antimicrobial peptides from bovine lactoferrin on the membranes of *Candida albicans* and *Escherichia coli*, Peptides 26 (2005) 1537–1542.
[30] E.F. Haney, F. Lau, H.J. Vogel, Solution structures and model membrane interactions of lactoferrampin, an antimicrobial peptide derived from bovine lactoferrin, Biochim. Biophys. Acta 1768 (2007) 2355–2364.
[31] E.F. Haney, K. Nazmi, J.G. Bolscher, H.J. Vogel, Influence of specific amino acid side-chains on the antimicrobial activity and structure of bovine lactoferrampin Biochem. Cell Biol., (in press) .
[32] E.F. Haney, K. Nazmi, F. Lau, J.G. Bolscher, H.J. Vogel, Novel lactoferrampin antimicrobial peptides derived from human lactoferrin, Biochimie 91 (2009) 141–154.
[33] J.G. Bolscher, R. Adao, K. Nazmi, P.A. van den Keybus, W. van 't Hof, A.V.N. Amerongen, M. Bastos, E.C. Veerman, Bactericidal activity of LFchimera is stronger and less sensitive to ionic strength than its constituent lactoferricin and lactoferrampin peptides, Biochimie 91 (2009) 123–132.

[34] N. Leon-Sicairos, A. Canizalez-Roman, M. de la Garza, M. Reyes-Lopez, J. Zazueta-Beltran, K. Nazmi, B. Gomez-Gil, J.G. Bolscher, Bactericidal effect of lactoferrin and lactoferrin chimera against halophilic *Vibrio parahaemolyticus*, Biochimie 91 (2009) 133–140.
[35] F. Lopez-Soto, N. Leon-Sicairos, K. Nazmi, J.G. Bolscher, M. de la Garza, Microbicidal effect of the lactoferrin peptides lactoferricin17–30, lactoferrampin265–284, and lactoferrin chimera on the parasite *Entamoeba histolytica*, Biometals 23 (2010) 563–568.
[36] H. Flores-Villasenor, A. Canizalez-Roman, M. Reyes-Lopez, K. Nazmi, M. de la Garza, J. Zazueta-Beltran, N. Leon-Sicairos, J.G. Bolscher, Bactericidal effect of bovine lactoferrin, LFcin, LFampin and LFchimera on antibiotic-resistant *Staphylococcus aureus* and *Escherichia coli*, Biometals 23 (2010) 569–578.
[37] M.H. Chiu, E.J. Prenner, Differential scanning calorimetry: an invaluable tool for a detailed thermodynamic characterization of macromolecules and their interactions, J. Pharm. Bioallied. Sci. 3 (2011) 39–59.
[38] H. Ulvatne, H.H. Haukland, O. Olsvik, L.H. Vorland, Lactoferricin B causes depolarization of the cytoplasmic membrane of *Escherichia coli* ATCC 25922 and fusion of negatively charged liposomes, FEBS Lett. 492 (2001) 62–65.
[39] D.J. Schibli, H.N. Hunter, V. Aseyev, T.D. Starner, J.M. Wiencek, P.B. McCray, B.F. Tack, H.J. Vogel, The solution structures of the human beta-defensins lead to a better understanding of the potent bactericidal activity of HBD3 against *Staphylococcus aureus*, J. Biol. Chem. 277 (2002) 8279–8289.
[40] B.N. Ames, E.F. Neufeld, V. Ginsberg, Assay of inorganic phosphate, total phosphate and phosphatases, Meth. Enzymol, Academic Press, New York, 1966, pp. 115–118.
[41] E.J. Prenner, R.N.A.H. Lewis, L.H. Kondejewski, R.S. Hodges, R.N. McElhaney, Differential scanning calorimetric study of the effect of the antimicrobial peptide gramicidin S on the thermotropic phase behavior of phosphatidylcholine, phosphatidylethanolamine and phosphatidylglycerol lipid bilayer membranes, Biochim. Biophys. Acta 1417 (1999) 211–223.
[42] G. Fujii, S. Horvath, S. Woodward, F. Eiserling, D. Eisenberg, A molecular model for membrane fusion based on solution studies of an amphiphilic peptide from HIV gp41, Protein Sci. 1 (1992) 1454–1464.
[43] R.W. Janes, B.A. Wallace, B.A. Wallace, R.W. Janes, An Introduction to Circular Dichroism and Synchrotron Radiation Circular Dichroism Spectroscopy, in: P.I. Haris (Ed.), Modern Techniques for Circular Dichroism and Synchrotron Radiation Circular Dichroism Spectroscopy, IOS Press, Amsterdam, 2009, pp. 1–18.
[44] L.T. Nguyen, D.I. Chan, L. Boszhard, S.A. Zaat, H.J. Vogel, Structure-function studies of chemokine-derived carboxy-terminal antimicrobial peptides, Biochim. Biophys. Acta 1798 (2010) 1062–1072.
[45] T.L. Hwang, A.J. Shaka, Water suppression that works — excitation sculpting using arbitrary wave-forms and pulsed-field gradients, J. Magn. Reson. A 112 (1995) 275–279.
[46] F. Delaglio, S. Grzesiek, G.W. Vuister, G. Zhu, J. Pfeifer, A. Bax, Nmrpipe — a multidimensional spectral processing system based on UNIX pipes, J. Biomol. NMR 6 (1995) 277–293.
[47] B.A. Johnson, Using NMRView to visualize and analyze the NMR spectra of macromolecules, Meth. Mol. Biol. 278 (2004) 313–352.
[48] K. Wuthrich, NMR of Proteins and Nucleic Acids, John Wiley & Sons Inc., New York, 1986.
[49] A.T. Brunger, P.D. Adams, G.M. Clore, W.L. Delano, P. Gros, R.W. Grosse-Kunstleve, J.S. Jiang, J. Kuszewski, M. Nilges, N.S. Pannu, R.J. Read, L.M. Rice, T. Simonson, G.L. Warren, Crystallography & NMR system: a new software suite for macromolecular structure determination, Acta Crystallogr. D: Biol. Crystallogr. 54 (1998) 905–921.
[50] J.P. Linge, S.I. O'Donoghue, M. Nilges, Automated assignment of ambiguous nuclear overhauser effects with ARIA, Nucl. Magn. Reson. Biol. Macromol. Part B 339 (2001) 71–90.
[51] R.A. Laskowski, J.A.C. Rullmann, M.W. MacArthur, R. Kaptein, J.M. Thornton, AQUA and PROCHECK-NMR: programs for checking the quality of protein structures solved by NMR, J. Biomol. NMR 8 (1996) 477–486.
[52] R. Koradi, M. Billeter, K. Wuthrich, MOLMOL: a program for display and analysis of macromolecular structures, J. Mol. Graph. 14 (1996) 51–55.
[53] L. Wang, M. Zhou, A. McClelland, A. Reilly, T. Chen, R. Gagliardo, B. Walker, C. Shaw, Novel dermaseptin, adenoregulin and caerin homologs from the Central American red-eyed leaf frog, Agalychnis callidryas, revealed by functional peptidomics of defensive skin secretion, Biochimie 90 (2008) 1435–1441.
[54] S.S. Kim, M.S. Shim, J. Chung, D.Y. Lim, B.J. Lee, Purification and characterization of antimicrobial peptides from the skin secretion of *Rana dybowskii*, Peptides 28 (2007) 1532–1539.
[55] J. Zhou, S. McClean, A. Thompson, Y. Zhang, C. Shaw, P. Rao, A.J. Bjourson, Purification and characterization of novel antimicrobial peptides from the skin secretion of *Hylarana guentheri*, Peptides 27 (2006) 3077–3084.
[56] X. Wang, Y.Z. Song, J.X. Li, H. Liu, X.Q. Xu, R. Lai, K.Y. Zhang, A new family of antimicrobial peptides from skin secretions of *Rana pleuraden*, Peptides 28 (2007) 2069–2074.
[57] V. Reshmy, V. Preeji, A. Parvin, K. Santhoshkumar, S. George, Three novel antimicrobial peptides from the skin of the Indian bronzed frog *Hylarana temporalis* (Anura: Ranidae), J. Pept. Sci. 17 (2011) 342–347.
[58] X. Liu, R. Liu, L. Wei, H. Yang, K. Zhang, J. Liu, R. Lai, Two novel antimicrobial peptides from skin secretions of the frog, *Rana nigrovittata*, J. Pept. Sci. 17 (2011) 68–72.
[59] M. Zasloff, Magainins, a class of antimicrobial peptides from *Xenopus* skin — isolation, characterization of 2 active forms, and partial cDNA sequence of a precursor, Proc. Natl. Acad. Sci. U. S. A. 84 (1987) 5449–5453.
[60] S. Cherry, N. Silverman, Host–pathogen interactions in Drosophila: new tricks from an old friend, Nat. Immunol. 7 (2006) 911–917.
[61] B. Lemaitre, J. Hoffmann, The host defense of *Drosophila melanogaster*, Annu. Rev. Immunol. 25 (2007) 697–743.
[62] R.E.W. Hancock, G. Diamond, The role of cationic antimicrobial peptides in innate host defences, Trends Microbiol. 8 (2000) 402–410.
[63] M. Tollin, P. Bergman, T. Svenberg, H. Jornvall, G.H. Gudmundsson, B. Agerberth, Antimicrobial peptides in the first line defence of human colon mucosa, Peptides 24 (2003) 523–530.
[64] D. Andreu, J. Ubach, A. Boman, B. Wahlin, D. Wade, R.B. Merrifield, H.G. Boman, Shortened cecropin A-melittin hybrids. Significant size reduction retains potent antibiotic activity, FEBS Lett. 296 (1992) 190–194.
[65] W.L. Maloy, U.P. Kari, Structure–activity studies on magainins and other host defense peptides, Biopolymers 37 (1995) 105–122.
[66] A. Giacometti, O. Cirioni, W. Kamysz, G. D'Amato, C. Silvestri, M.S. Del Prete, J. Lukasiak, G. Scalise, In vitro activity and killing effect of the synthetic hybrid cecropin A-melittin peptide CA(l–7)M(2–9)NH2 on methicillin-resistant nosocomial isolates of *Staphylococcus aureus* and interactions with clinically used antibiotics, Diagn. Microbiol. Infect. Dis. 49 (2004) 197–200.
[67] A. Giacometti, O. Cirioni, W. Kamysz, G. D'Amato, C. Silvestri, M.S. Del Prete, J. Lukasiak, G. Scalise, Comparative activities of cecropin A, melittin, and cecropin A-melittin peptide CA(1–7)M(2–9)NH2 against multidrug-resistant nosocomial isolates of *Acinetobacter baumannii*, Peptides 24 (2003) 1315–1318.
[68] J.M. Saugar, M.J. Rodriguez-Hernandez, B.G. de la Torre, M.E. Pachon-Ibanez, M. Fernandez-Reyes, D. Andreu, J. Pachon, L. Rivas, Activity of cecropin A-melittin hybrid peptides against colistin-resistant clinical strains of *Acinetobacter baumannii*: molecular basis for the differential mechanisms of action, Antimicrob. Agents Chemother. 50 (2006) 1251–1256.
[69] W. Hongbiao, N. Baolong, X. Mengkui, H. Lihua, S. Weifeng, M. Zhiqi, Biological activities of cecropin B-thanatin hybrid peptides, J. Pept. Res. 66 (2005) 382–386.
[70] K. Wakamatsu, A. Takeda, T. Tachi, K. Matsuzaki, Dimer structure of magainin 2 bound to phospholipid vesicles, Biopolymers 64 (2002) 314–327.
[71] F. Porcelli, B.A. Buck-Koehntop, S. Thennarasu, A. Ramamoorthy, G. Veglia, Structures of the dimeric and monomeric variants of magainin antimicrobial peptides (MSI-78 and MSI-594) in micelles and bilayers, determined by NMR spectroscopy, Biochemistry 45 (2006) 5793–5799.
[72] Y. Mukai, Y. Matsushita, T. Niidome, T. Hatekeyama, H. Aoyag, Parallel and antiparallel dimers of magainin 2: their interaction with phospholipid membrane and antibacterial activity, J. Pept. Sci. 8 (2002) 570–577.
[73] S.B. Tencza, D.J. Creighton, T. Yuan, H.J. Vogel, R.C. Montelaro, T.A. Mietzner, Lentivirus-derived antimicrobial peptides: increased potency by sequence engineering and dimerization, J. Antimicrob. Chemother. 44 (1999) 33–41.
[74] P.C. Dewan, A. Anantharaman, V.S. Chauhan, D. Sahal, Antimicrobial action of prototypic amphipathic cationic decapeptides and their branched dimers, Biochemistry 48 (2009) 5642–5657.
[75] S.T. Yang, J.I. Kim, S.Y. Shin, Effect of dimerization of a beta-turn antimicrobial peptide, PST13-RK, on antimicrobial activity and mammalian cell toxicity, Biotechnol. Lett. 31 (2009) 233–237.
[76] W. Hoffmann, K. Richter, G. Kreil, A novel peptide designated PYLa and its precursor as predicted from cloned messenger-RNA of *Xenopus laevis* skin, EMBO J. 2 (1983) 711–714.
[77] H.V. Westerhoff, M. Zasloff, J.L. Rosner, R.W. Hendler, A. De Waal, A. Vaz Gomes, P.M. Jongsma, A. Riethorst, D. Juretic, Functional synergism of the magainins PGLa and magainin-2 in *Escherichia coli*, tumor cells and liposomes, Eur. J. Biochem. 228 (1995) 257–264.
[78] R.W. Williams, R. Starman, K.M. Taylor, K. Gable, T. Beeler, M. Zasloff, D. Covell, Raman spectroscopy of synthetic antimicrobial frog peptides magainin 2a and PGLa, Biochemistry 29 (1990) 4490–4496.
[79] E.F. Haney, H.J. Vogel, G.A. Webb, NMR of Antimicrobial Peptides, in: Annual Reports on NMR Spectroscopy, Academic Press, Burlington, 2009 pp. 1–51.
[80] M. Schwaiger, M. Lebendiker, H. Yerushalmi, M. Coles, A. Groger, C. Schwarz, S. Schuldiner, H. Kessler, NMR investigation of the multidrug transporter EmrE, an integral membrane protein, Eur. J. Biochem. 254 (1998) 610–619.
[81] M.E. Girvin, R.H. Fillingame, Helical structure and folding of subunit c of F1F0 ATP synthase: 1H NMR resonance assignments and NOE analysis, Biochemistry 32 (1993) 12167–12177.
[82] M.E. Girvin, V.K. Rastogi, F. Abildgaard, J.L. Markley, R.H. Fillingame, Solution structure of the transmembrane H+-transporting subunit c of the F1F0 ATP synthase, Biochemistry 37 (1998) 8817–8824.
[83] O.Y. Dmitriev, K.H. Freedman, J. Hermolin, R.H. Fillingame, Interaction of transmembrane helices in ATP synthase subunit a in solution as revealed by spin label difference NMR, Biochim. Biophys. Acta 1777 (2008) 227–237.
[84] M. Buck, Trifluoroethanol and colleagues: cosolvents come of age. Recent studies with peptides and proteins, Q. Rev. Biophys. 31 (1998) 297–355.
[85] M. Zhang, T. Yuan, H.J. Vogel, A peptide analog of the calmodulin-binding domain of myosin light chain kinase adopts an alpha-helical structure in aqueous trifluoroethanol, Protein Sci. 2 (1993) 1931–1937.
[86] M.R. de Planque, B.B. Bonev, J.A. Demmers, D.V. Greathouse, R.E. Koeppe II, F. Separovic, A. Watts, J.A. Killian, Interfacial anchor properties of tryptophan residues in transmembrane peptides can dominate over hydrophobic matching effects in peptide–lipid interactions, Biochemistry 42 (2003) 5341–5348.
[87] W.M. Yau, W.C. Wimley, K. Gawrisch, S.H. White, The preference of tryptophan for membrane interfaces, Biochemistry 37 (1998) 14713–14718.
[88] I. Daidone, A. Magliano, A. Di Nola, G. Mignogna, M.M. Clarkson, A.R. Lizzi, A. Oratore, F. Mazza, Conformational study of bovine lactoferricin in membrane-micking conditions by molecular dynamics simulation and circular dichroism, Biometals 24 (2011) 259–268.

[89] M. Arseneault, S. Bedard, M. Boulet-Audet, M. Pezolet, Study of the interaction of lactoferricin B with phospholipid monolayers and bilayers, Langmuir 26 (2010) 3468–3478.
[90] M. Bastos, T. Silva, V. Teixeira, K. Nazmi, J.G. Bolscher, S.S. Funari, D. Uhrikova, Lactoferrin-derived antimicrobial Peptide induces a micellar cubic phase in a model membrane system, Biophys. J. 101 (2011) L20–L22.
[91] F. Porcelli, R. Verardi, L. Shi, K.A. Henzler-Wildman, A. Ramamoorthy, G. Veglia, NMR structure of the cathelicidin-derived human antimicrobial peptide LL-37 in dodecylphosphocholine micelles, Biochemistry 47 (2008) 5565–5572.
[92] T.J. Park, J.S. Kim, H.C. Ahn, Y. Kim, Solution and solid-state NMR structural studies of antimicrobial peptides LPcin-I and LPcin-II, Biophys. J. 101 (2011) 1193–1201.
[93] J.K. Kim, E. Lee, S. Shin, K.W. Jeong, J.Y. Lee, S.Y. Bae, S.H. Kim, J. Lee, S.R. Kim, D.G. Lee, J.S. Hwang, Y. Kim, Structure and function of papiliocin with antimicrobial and anti-inflammatory activities isolated from the swallowtail butterfly, Papilio xuthus, J. Biol. Chem. 286 (2011) 41296–41311.
[94] R.S. Prosser, F. Evanics, J.L. Kitevski, M.S. Al-Abdul-Wahid, Current applications of bicelles in NMR studies of membrane-associated amphiphiles and proteins, Biochemistry 45 (2006) 8453–8465.
[95] E. Salnikov, C. Aisenbrey, V. Vidovic, B. Bechinger, Solid-state NMR approaches to measure topological equilibria and dynamics of membrane polypeptides, Biochim. Biophys. Acta 1798 (2010) 258–265.
[96] E. Matyus, C. Kandt, D.P. Tieleman, Computer simulation of antimicrobial peptides, Curr. Med. Chem. 14 (2007) 2789–2798.
[97] H.J. Vogel, D.J. Schibli, W. Jing, E.M. Lohmeier-Vogel, R.F. Epand, R.M. Epand, Towards a structure–function analysis of bovine lactoferricin and related tryptophan- and arginine-containing peptides, Biochem. Cell Biol. 80 (2002) 49–63.
[98] H.H. Haukland, H. Ulvatne, K. Sandvik, L.H. Vorland, The antimicrobial peptides lactoferricin B and magainin 2 cross over the bacterial cytoplasmic membrane and reside in the cytoplasm, FEBS Lett. 508 (2001) 389–393.
[99] H. Ulvatne, O. Samuelsen, H.H. Haukland, M. Kramer, L.H. Vorland, Lactoferricin B inhibits bacterial macromolecular synthesis in *Escherichia coli* and *Bacillus subtilis*, FEMS Microbiol. Lett. 237 (2004) 377–384.